Journal of Structural Geology, Vol. 2, No. 1/2, pp. 101 to 109.
Pergamon Press Ltd. 1980. Printed in Great Britain.

0191-8141/80/0601-0101 $02.00/0

Rotation and deformation of randomly oriented planar and linear structures in progressive simple shear

L. SKJERNAA
Institute of General Geology, Østervoldgade 10, DK-1350 Copenhagen K, Denmark

(*Received* 17 *May* 1979; *accepted in revised form* 7 *August* 1979)

Abstract—A mathematical solution is presented of how randomly oriented planes and lines are rotated and deformed during progressive homogeneous simple shear. The results are used to predict the redistribution and modification of pre-shear folds. For most initial orientations very large shears ($\gamma = 20$ or more) are required to make the fold axes subparallel to the *a*-axis of the simple shear deformation.

During progressive deformation the principal axes of the two-dimensional strain in a randomly oriented plane rotate, both in relation to the kinematic axes and in relation to material lines included in the plane. This may result in very complicated structures when competent layers are involved in the deformation. Combinations of superimposed fold and boudinage structures, with orientations highly dependent on the initial orientation of the layer, are to be expected.

INTRODUCTION

IT IS well known that shear zones in isotropic rocks develop a cleavage, schistosity or foliation parallel to the *XY*-plane of the finite strain ellipsoid, and often a very strong stretching lineation parallel to the *X*-direction.

Many shear zones cut through terrains which already possess planar and linear structural elements with various orientations. An example is a folded or multiple folded gneiss terrain. As the pre-shearing structural elements are not in general symmetric with the kinematic axes of the simple shear deformation, it is necessary to deal with their rotation and deformation in three dimensions.

Medium scale structures, in the form of folds and/or boudinage structures, are very common in major shear zones. The folds may be of the compositional layering, which may or may not parallel the *XY*-plane, but folded dykes and discordant or concordant quartz veins or quartzo-feldspathic veins are also common. Quite commonly these folds are combined with boudinage structures, but the distance between single boudins may be so large as to make it difficult to reconstruct the original layer.

The structures may have formed either prior to shearing or as a consequence of simple shear deformation, either from buckle folding and/or boudinage of competent layers involved in the deformation, or by inhomogeneities in the simple shear. Stretching lineations may be parallel to the layer and the maximum finite stretching directions in the surface of the layer, not the *X*-direction of the bulk finite strain. Similarly, intersection lineations parallel to the intersections between layer surfaces and shear plane, are not parallel to the *Y*-direction.

The rotation and deformation of planar and linear structures in irrotational deformations was thoroughly treated by Flinn (1962) and later discussed by Ramsay (1967) and by Talbot (1970).

This article presents a mathematical solution for the reorientation and deformation of pre-shear zone planes and lines during the formation of a shear zone by simple shear, and some models for the initiation and progressive development of contemporaneous shear zone structures. The practical application of this theory will be described in a later paper about medium scale structures and their orientations within a major Precambrian shear zone in southeast Norway, already mentioned by Skjernaa (1972).

PROGRESSIVE HOMOGENEOUS SIMPLE SHEAR

Rotation of planes

The spatial orientations of a plane *P* in relation to the kinematic axes *a*, *b* and *c* of a progressive simple shear deformation, can be described by the angles v ($0 \leq v < 180$) and p ($0 \leq p < 180$) (Figs. 1a & b). The plane will rotate during the deformation around its line of intersection with the shear plane. The angle v will remain unchanged, while p changes to p'. For a certain amount of shear, given by the value of γ, p' is given by equation (2) of the Appendix. A diagram giving p' as a

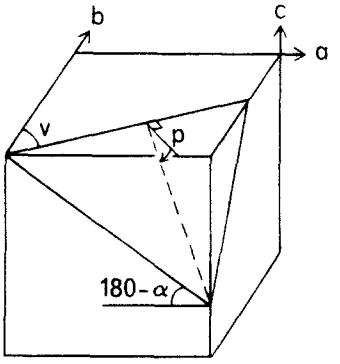

Fig. 1. (a) Localisation of the angles v and p which define the orientation of a plane.

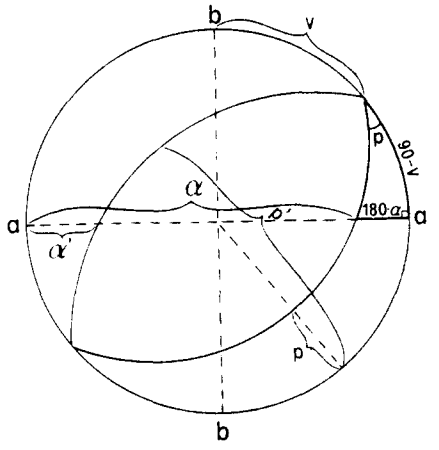

Fig. 1. (b) Stereographic lower hemisphere projection showing the rotation of a plane (v, p) to a position (v', p').

function of v and p has been constructed for $\gamma = 4$ (Fig. 2). It is seen that the amount of rotation increases as v approaches 180 (see also Figs. 7b–f). Planes having small values of p will only rotate slightly for low values of γ, but for high shears they will rotate more, except when v is close to 90.

As an example a plane with initial orientation $v = 30$, $p = 4$ will have have $p' = 10.05$ for $\gamma = 10$ but $p' = 161.68$ for $\gamma = 20$ and $p' = 178.03$ for $\gamma = 50$. However, a plane with $v = 30$, $p = 1$ will rotate much less: $p' = 1.18$ for $\gamma = 10$, $p' = 1.43$ for $\gamma = 20$ and $p' = 4.09$ for $\gamma = 50$.

The largest possible rotation ($p'-p$) is taken up by the plane having the initial orientation (v, p) = (0, $2\theta'$) where $2\theta'$ is the angle between the shear plane and the other plane of no finite longitudinal strain in the strain ellipsoid. It will end up having the orientation (v, p) = (0, 180–$2\theta'$), and then have been rotated through an angle 180–$4\theta'$. $2\theta' = \tan^{-1}\frac{2}{\gamma}$ (Ramsay & Graham 1970 equation 36).

A mathematical solution for the reorientation of planes in a simple shear deformation, is also given by Carreras (1975) and Owens (1972). A magnificent example of such reorientations is described from the Nagssugtoqidian shear belt in West Greenland by Escher *et al.* (1975).

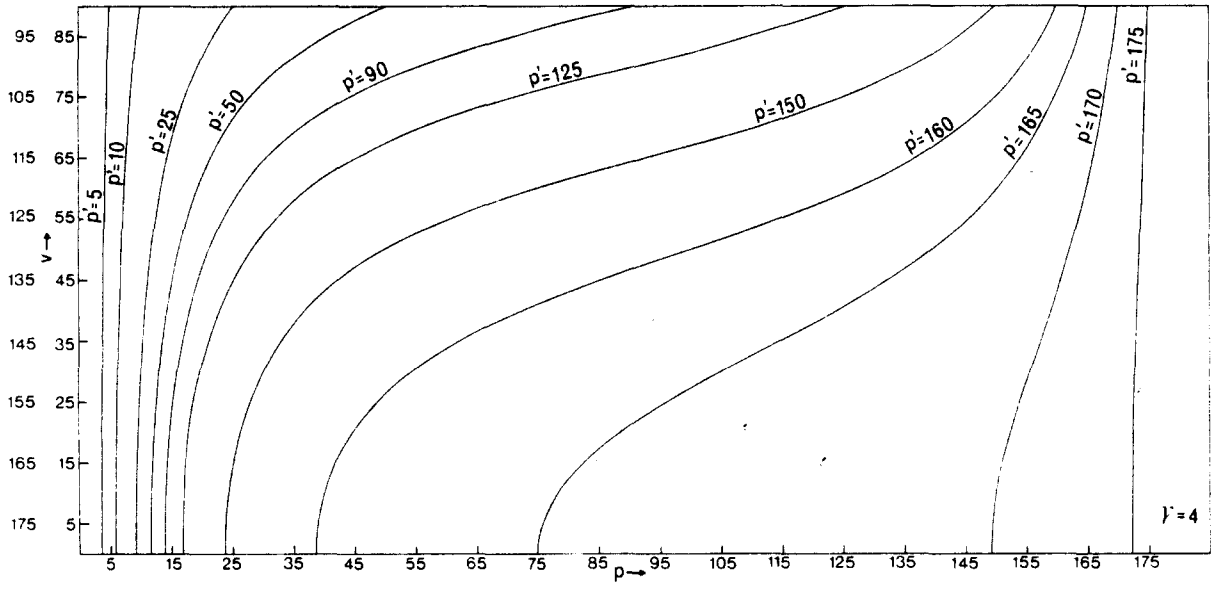

Fig. 2. Diagram showing p' as a function of v and p after a simple shear of $\gamma = 4$.

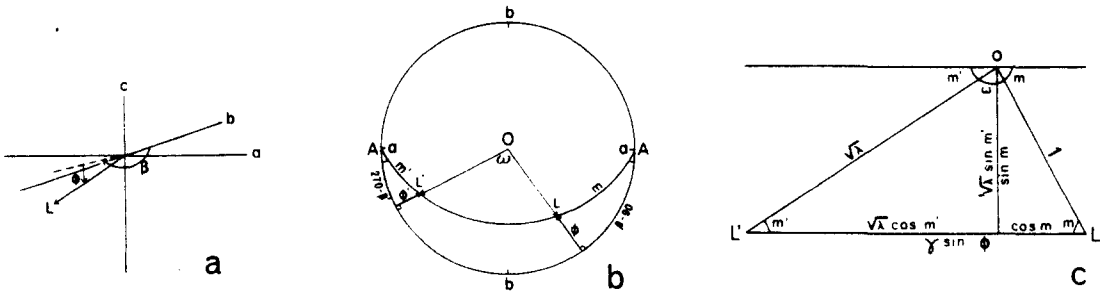

Fig. 3. (a) Localisation of the angles β and φ which define the orientation of a line. (b) Stereographic projection showing the rotation of a line L (β, φ) to a position L' (β', φ'). (c) Triangle OLL' from Fig. 3(b).

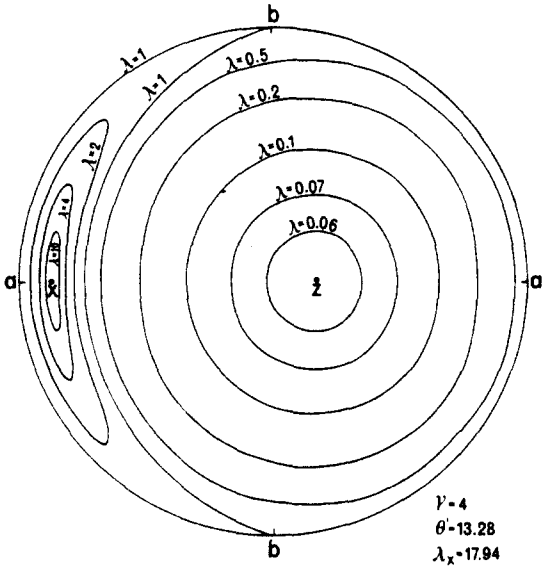

Fig. 4.

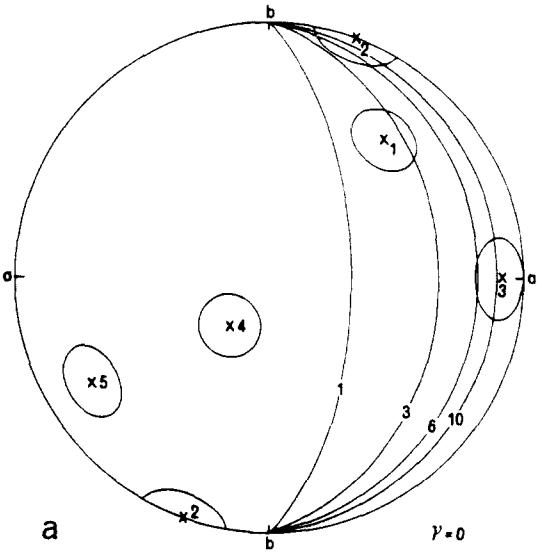

Fig. 5(a).

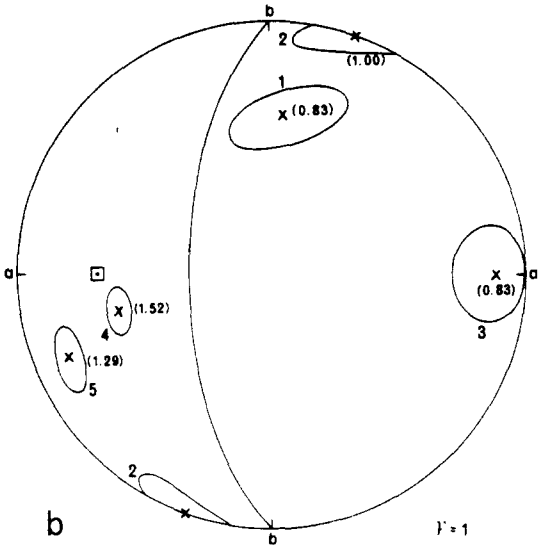

Fig. 5(b).

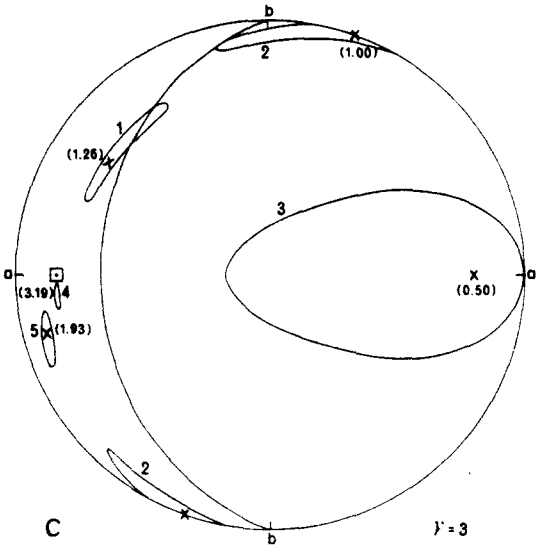

Fig. 5(c).

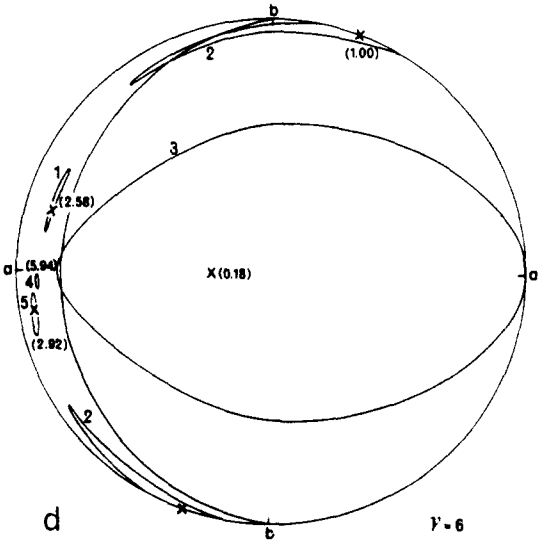

Fig. 5(d).

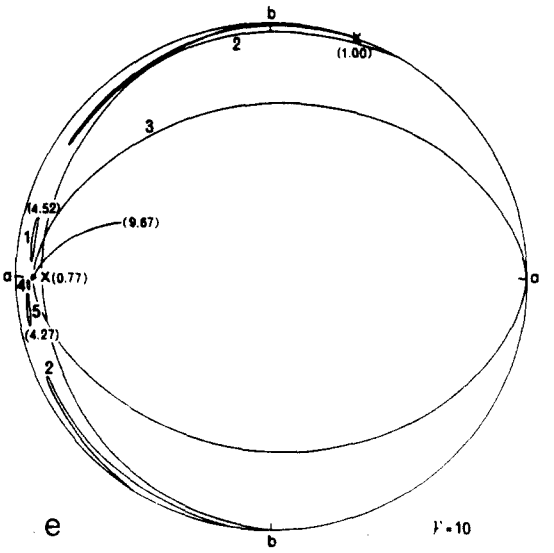

Fig. 5(e).

Fig. 4. Stereographic projection showing a series of cones, each of which contains all the lines that have been elongated by a certain amount given by the values of λ.

Fig. 5(a–e). Rotation of pre-shearing lineations with initial orientations confined by cones 1–5, 5(a). The numbers in brackets are values of $\sqrt{\lambda}$ giving the elongation of the original central line of the cones. The great circles in (a) describe the planes which after a certain shear (γ indicated by the numbers) will have rotated to a position where they separate into the extension and shortening fields. These positions are those of the λ = 1 great circles in Figs. (b–e). The squares mark the orientation of the *X*-axis.

Rotation and elongation of lines

A line L having an initial orientation in relation to the kinematic axes given by β ($0 \leq \beta \leq 360$) and φ ($0 \leq \varphi \leq 90$) (Fig. 3a) and an initial length l (Figs. 3b & c), will during the deformation rotate in the plane containing the line L and the a-axis through an angle ω, and at the same time change its length. Lines initially oriented such that $0 < \beta < 180$ will shorten in the beginning. But as they pass the bc-plane during their rotation they will start to stretch. Lines with $180 \leq \beta \leq 360$ will be stretched during the whole deformation.

The final position (β', φ') and the final length $\sqrt{\lambda}$ for a certain amount of shear, is given by the equations (11), (10) and (9) of the Appendix.

All the lines that have been equally elongated after a certain amount of shear are contained within the surface of a cone given by equation (17) of the Appendix. A Lambert-net projection showing a series of such cones for $\gamma = 4$ is given in Fig. 4. If the curves on Fig. 4 are looked upon as contours, they give the shape of the lower half of the deformation ellipsoid (notice that the values given are quadratic elongations). The diagram is divided by the two great circles describing the $\lambda = 1$ planes into an extension field and a shortening field.

The angle ω through which a line has rotated during the deformation (Figs. 3b & c) is given by equation (18) of the Appendix.

The distribution of lines will be such that during deformation all lines which initially lay between the shear plane and the plane with orientation (v, p) = (0, $2\theta'$) will spread over the shortening field, while lines with other initial orientations will be concentrated into the stretching field and at the two $\lambda = 1$ planes.

Examples of the rotation and spread/concentration of lines during successive stages of the deformation are given in Figs. 5(a– e). Five groups of lineations, which for $\gamma = 0$ are bounded by cones with a radius of 10°, have been chosen to illustrate the influence of the initial orientation on various distribution patterns arrived at for certain shears. Each of the groups could for a particular shear zone define the orientation of fold axes related to pre-shearing folding.

The modification of angular density distribution of lines during simple shear deformation is not discussed here in any detail. It is described by Owens (1972).

It is seen from Figs. 5(a–e) that although all lines, except those lying in the shear plane, rotate towards the shear direction, they never approach close to this direction even for large shears. For large strains group 2 lineations plot close to a great circle, but this neither defines the shear plane nor the XY-plane.

Examples of rotation of pre-shear fold axes are given by Bak *et al.* (1975) from Greenland, and by Pecher (1977) from the Himalayas.

Two-dimensional strain in a randomly oriented plane

A plane P, having the initial orientation (v, p) which is deformed to the orientation (v, p') (Fig. 1b), will, unless

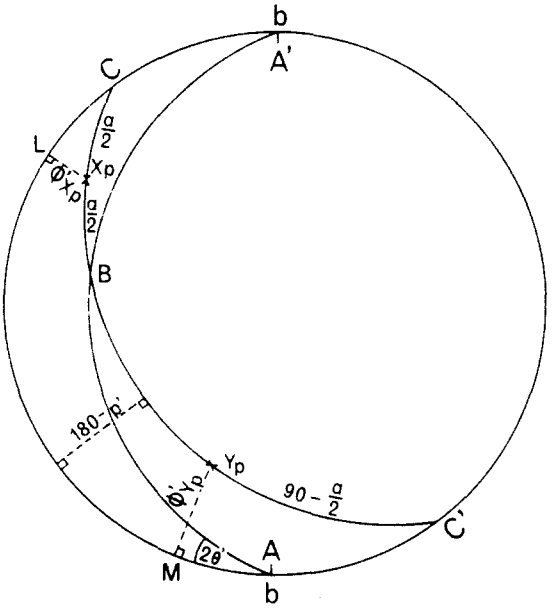

Fig. 6. Position of the strain axes X_P and Y_P in a rotated and internally deformed plane CBC'. For further explanation see text.

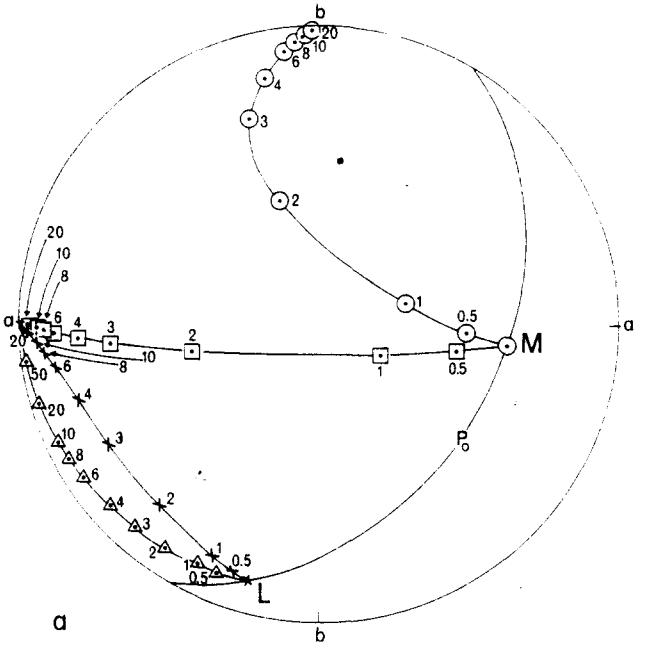

Fig. 7 (a) Orientations of the X_p axes (crosses) and Y_p axes (circles) in a plane P with initial position P_0 (v, p) = (30, 40) for different values of γ indicated by the numbers. The orientations of the material lines L and M, initially paralleling X_{P_i} and Y_{P_i} for the first increment of shear, are shown by triangles and squares.

$v = 0$, cross both the extension field and the shortening field of the finite strain ellipsoid, and thus be extended in some directions and shortened in others. The orientations of the maximum finite extension and shortening axes X_P and Y_P in the plane, at a given value of γ, are found as the mid-points of those parts of the great circle for the plane which falls within the extension field and the shortening field respectively (Figs. 4 and 6). The orientations are given by equations (23)–(27) of the Appendix.

Table 1. Length of the principal strain axes X_p and Y_p in the planes shown in Figs. 7(a–f) and thickness t of layers with initial thickness 1

	Plane 1 (v, p) = (30, 40) $\sqrt{\lambda_{X_P}}/\sqrt{\lambda_{Y_P}}/t$	Plane 2 (v, p) = (40, 130) $\sqrt{\lambda X_p}/\sqrt{\lambda_{Y_P}}/t$	Plane 3 (v, p) = (150, 5.37) $\sqrt{\lambda_{X_P}}/\sqrt{\lambda_{Y_P}}/t$	Plane 4 (v, p) = (70, 171.3) $\sqrt{\lambda_{X_P}}/\sqrt{\lambda_{Y_P}}/t$	Plane 5 (v, p) = (90, 60) $\sqrt{\lambda_{X_P}}/\sqrt{\lambda_{Y_P}}/t$	Plane 6 (v, p) = (80, 30) $\sqrt{\lambda_{X_P}}/\sqrt{\lambda_{Y_P}}/t$	Plane 7 (v, p) = (0, 90) $\sqrt{\lambda_{X_P}}/\sqrt{\lambda_{Y_P}}/t$
$\gamma = 1$	1.08/0.63/1.48	1.58/0.92/0.69	1.01/0.91/1.09	1.10/0.96/0.95	1.52/0.66/1.00	1.24/0.74/1.08	1.41/1.00/0.71
$\gamma = 3$	1.64/0.67/0.90	2.97/0.85/0.40	1.02/0.76/1.29	1.30/0.88/0.88	2.94/0.34/1.00	1.90/0.41/1.27	3.16/1.00/0.32
$\gamma = 6$	3.34/0.80/0.38	5.19/0.81/0.24	1.05/0.49/1.93	1.64/0.79/0.78	5.38/0.19/1.00	3.17/0.19/1.65	6.08/1.00/0.16
$\gamma = 10$	5.84/0.83/0.21	8.22/0.80/0.15	1.11/0.19/4.82	2.12/0.70/0.68	8.77/0.11/1.00	5.05/0.10/2.00	10.05/1.00/0.10

During the progressive deformation the X_P and Y_P axes will change their position, not only in relation to the *abc*-kinematic-axes, but also in relation to material lines, defined as lines attached to material points, within the plane. While the material lines rotate in the plane containing the line and the *a*-axis, the X_P and Y_P directions rotate in a much more complicated manner towards the *a*- and *b*-axes respectively. Figure 7(a) shows these relations for a general case, in which the initial orientations of lines L and M are parallel to X_{Pi} and Y_{Pi} for the first incremental shear in plane P_0. In this general case very large shear strains, about 20 or more, are required to make the lines L and M and the X_P direction subparallel to the *a*-axis, and the Y_P direction subparallel to the *b*-axis. Figures 7(b–f) illustrate the rotation of seven selected planes and the position of X_P and Y_P axes within them at successive stages of deformation. The values of finite stretching and shortening parallel to the X_P and Y_P axes are given in Table 1, together with the finite elongation t normal to the planes [given by

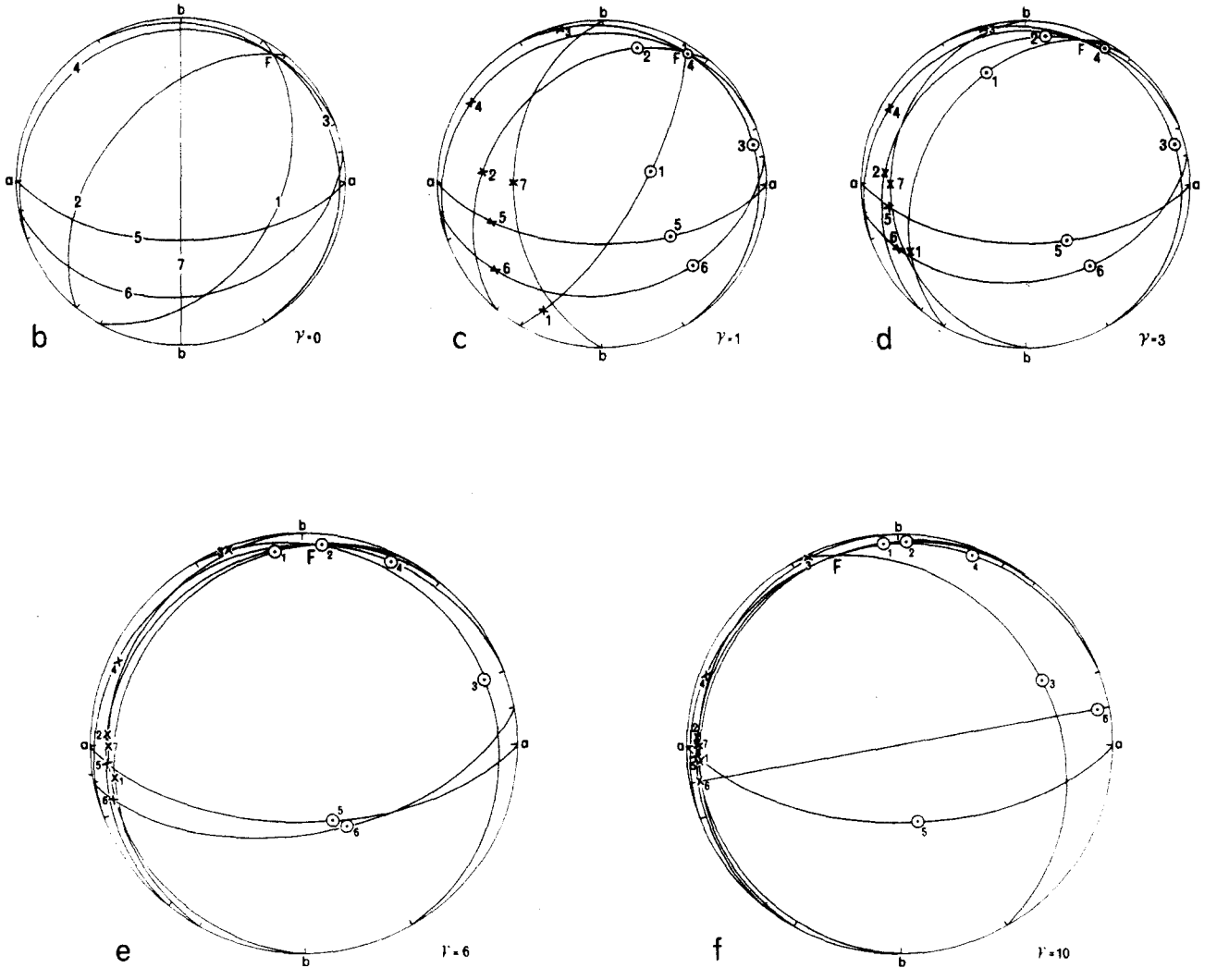

Fig. 7 (b–f) Rotation of seven selected planes (1–7) and positions of the internal strain axes X_p (crosses) and Y_p (circles) in the planes at different stages of deformation. Plane 1 is identical to plane P in (a).

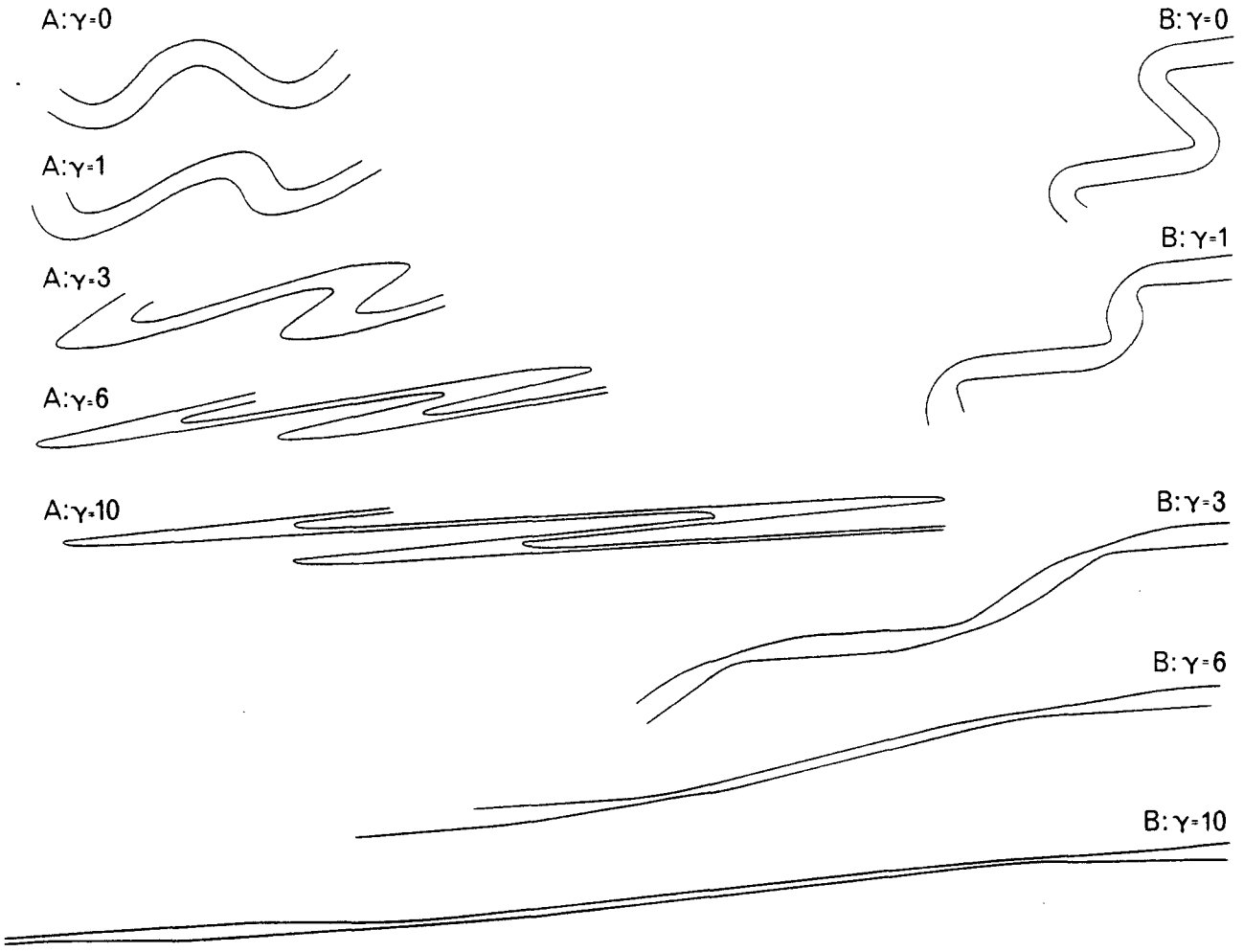

Fig. 8. Profiles through folds which include planes 1–4 (A) or planes 1, 2 and 4 (B) in their surfaces, and which initially ($\gamma = 0$) have constant layer thickness. The profile planes change their material position from one increment of deformation to the next. The trace of the shear planes is horizontal in all the profiles.

equation (28) of the Appendix].

Four of the planes (1, 2, 3 and 4) intersect each other in a line F, which could describe a fold axis. Figure 8 shows the change of shapes, seen in profiles, of two folds which have fold axes parallel to F. Fold A includes in its folded surface planes 1 and 2 in the limbs and 3 and 4 in the hinge zone. Fold B includes planes 1 and 4 in the limbs and plane 2 in the hinge zone. While fold A becomes more and more tightened and overturned during the deformation, fold B is unrolled. Note how fold B could easily be mistaken for a folded pinch-and-swell structure, especially where $\gamma = 1$ and $\gamma = 3$.

Bak *et al.* (1975) have illustrated the change of style, seen in the *ac*-plane, of some very complicated folds which are redeformed by simple shear.

BULK HOMOGENEOUS PROGRESSIVE SIMPLE SHEAR AFFECTING COMPETENT LAYERS

As all planes, except those containing the *b*-axis, cross both the shortening and stretching fields of the finite and infinitesimal strain ellipsoids, the condition for the formation of both boudinage-structures and buckle folds are fulfilled when competent layers are involved in the deformation. Manz & Wickham (1978) have described some model experiments on buckle folding during simple shear deformation. However in all their models the competent layer paralleled the *b*-axis of the deformation.

For randomly oriented layers the orientations of the buckle fold axes and boudins are however far from obvious.

If the fold axes were thought to be perpendicular to the maximum finite shortening direction parallel with the surface of the layer, and the boudins perpendicular to the maximum finite extension direction, this would imply that they changed their material position throughout the deformation. This is obviously not the case for boudins and also seems rather doubtful for the fold axes. Possibly the folds are initiated with their axes paralleling the X_P direction, but from the time of initiation, or from some stage of amplification, they may rotate as material lines (Fig. 7a). This was also suggested by Escher & Watterson (1974). Such a rotation mechanism implies that the resulting axial direction depends on the time of initiation of the folds, or the time when the folds reached a certain amplitude.

The generation and subsequent rotation and flattening of contemporaneous buckle folds have been described by Williams (1978), who however considers them to be rotating within the XY-plane (the schistosity plane) of the strain ellipsoid.

Model experiments suggest that buckle folds are not initiated simultaneously throughout the competent layer (Cobbold 1976), but that one fold is formed in a place where the layer had a suitable initial heterogeneity, and the subsequent folding spread out to both sides from the first formed fold. If this is true for the present type of deformation, folds with varying axial directions would be expected. The orientation of the first formed fold may however to some extent guide the orientation of the subsequent folds.

As for the boudins, their orientation may parallel the Y_P axis at some time between the initial pinching and the final separation, but from this stage they rotate as material lines. The final orientation of the boudin is highly dependent on the time where it starts to rotate as a material line (see Fig. 7a).

Whether a certain layer develops both boudinage and buckle fold structures, and which of these predates the other, is dependent on the initial orientation of the layer, and other factors (see Talbot 1970).

A layer parallel to P_0 in Fig. 7(a), and to plane 1 in Figs. 7(b–f), will at the beginning of the deformation undergo a low extension in the X_P direction, but a relatively large shortening in the Y_P direction (see Table 1). This may result in buckle folds with axes subparallel to L (Fig. 7a). These folds amplify and change shape during the next part of the deformation. As the stretching parallel to X_P becomes greater, boudinage at a high angle to the fold axes may result. Between $\gamma = 1$ and $\gamma = 2$ the direction normal to the fold axes (parallel with the surface of the layer) shifts from a progressive shortening to a progressive extension. This may cause the folds to partly unroll. Also, as the long directions of the boudins pass the bc-plane during their rotation, they become progressively stretched, and consequently boudinage at a high angle to the first formed boudins may occur.

The final result is chocolate-block boudinage with folds or remnants of folds preserved in the individual boudins.

A layer parallel to plane 5 (Figs. 7b–f) is continously extended parallel to X_P and shortened parallel to Y_P throughout the deformation. As the thickness of the layer is constant (the elongation normal to the layer surface is zero, Table 1), the layer may boudinage and the boudins may be folded sideways (in the plane of the layer) with axes more or less perpendicular to the layer.

Similar interpretations could be given to the other planes in Figs. 7(b–f). In some cases superimposed folds may form. This may happen if the first formed folds are rotated so far away from the normal to the infinitesimal shortening direction of the layer, and the folds are tightened and overturned so much, that continued shortening can no longer be accommodated by the folds.

CONCLUSION

It is concluded that although a simple shear deformation gives rise to a bulk plane strain, the structures in a shear zone should, in general, always be analysed in three dimensions.

The type, style and orientation of medium scale structures in a shear zone, are highly dependent on the initial orientation of pre-existing planes. This is especially so when the structures develop as a consequence of rheological contrasts between the deformed layer (or dyke or vein) and the host rock. A great variety of structures such as boudins, chocolate-block boudins, folds and superimposed folds and combinations of these, may be expected, even within a single layer.

The post-shear distribution and style of pre-shear folds, are similarly dependent on their original orientation. Very large strains are generally required to make both pre- and syn-shear linear structural elements subparallel with the a-axis in a simple shear deformation.

On the basis of theories and models proposed in this article and when the orientations of slip folds are also taken into consideration, the old discussion (see Kvale 1953 and Rhodes & Gayer 1977 for further references) as to whether the linear structures in shear zones are a or b structures seems rather meaningless.

Acknowledgements—Thanks are due to J. Myers who improved the English text, to Max Schierling who drafted the figures, and to H. Micheelsen for his advice in the preparation of computer programmes. Furthermore to Hans Ramberg, who, after the submission of this paper, drew my attention to a study of similar problems (Ramberg & Ghosh 1977), which I had not formerly been aware of.

REFERENCES

Bak, J. & Korstgård, J. & Sørensen, K. 1975. A major shear zone within the Nagssugtoqidian of West Greenland. *Tectonophysics* **27**, 191–209.

Carreras, J. 1975. Determinación de las relaciones angulares y de la deformación por cizalla, para cizallamientos en materiales con una heterogeneidad planar. *Acta Geol. Hispánica* **10**, 141–145.

Cobbold, P. 1976. Fold shapes as functions of progressive strain. *Phil. Trans. R. Soc.* **A283**, 129–138.

Escher, A. & Watterson, J. 1974. Stretching fabric, folds and crustal shortening. *Tectonophysics* **22**, 223–231.

Escher, A. & Escher, J. C. & Watterson, J. 1975. The reorientation of the Kangamiut Dike Swarm, West Greenland. *Can. Jl Earth Sci.* **12**, 158–173.

Flinn, D. 1962. On folding during three-dimensional progressive deformation. *Q. Jl geol. Soc. Lond.* **118**, 385–433.

Kvale, K. 1953. Linear structures and their relation to movement in the Caledonides of Scandinavia and Scotland. *Q. Jl geol. Soc. Lond.* **109**, 51–74.

Manz, R. & Wickham, J. 1978. Experimental analysis of folding in simple shear. *Tectonophysics* **44**, 79–90.

Owens, W. H. 1972. Strain Modification of angular density distributions. *Tectonophysics* **16**, 249–261.

Pecher, A. 1977. Geology of the Nepal Himalayas: Deformation and petrography in the main central thrust zone. *Colloques internationaux du C.N.R.S. No. 268 Écologie et Géologie de l'Himalaya.*

Ramberg, H. & Ghosh, K. 1977. Rotation and strain of linear and planar structures in three-dimensional progressive deformations. *Tectonophysics* **40**, 309–337.

Ramsay, J. G. 1967. *Folding and Fracturing of Rocks.* McGraw-Hill, New York.

Ramsay, J. G. & Graham, R. H. 1970. Strain variation in shear belts. *Can. J. Earth Sci.* **7**, 786–813.

Rhodes, S. & Gayer, R. A. 1977. Non-cylindrical folds, linear structures in the *X*-direction and mylonite developed during translation of the Caledonian Kalak Nappe Complex of Finmark. *Geol. Mag.* **114**, 329–341.

Skjernaa, L. 1972. The discovery of a regional crush belt in the Ørje area, southeast Norway. *Norsk geol. Tidsskr.* **52**, 459–461.

Talbot, C. J. 1970. The minimum strain ellipsoid using deformed quartz veins. *Tectonophysics* **9**, 47–76.

Williams, G. D. 1978. Rotation of contemporaneous folds into the *X* direction during overthrust processes in Laksefjord, Finmark. *Tectonophysics* **48**, 29–40.

APPENDIX

ROTATION OF PLANES

From the spherical triangle shown in Fig. 1(b):

$$\tan\alpha = -\tan p|\cos v| \text{ and } \tan\alpha' = -\tan p'|\cos v|. \quad (1)$$

α and α' are the angles in the undeformed and deformed state between the *a*-axis and the line of intersection between the plane *P* and the *ac*-plane.

Now, $\frac{1}{\tan\alpha'} = \frac{1}{\tan\alpha} + \gamma$ (Ramsay 1967, p. 88).

By substituting the values from (1) into this equation and replacing $\frac{1}{\tan p}$ with $-\tan(p-90)$ we arrive at:

$$p' = \tan^{-1}(\tan(p-90) + \gamma|\cos v|) + 90. \quad (2)$$

ROTATION AND ELONGATION OF LINES

From Fig. 3(b):

$$\sin A = \frac{\sin\varphi}{\sin m} = \frac{\sin\varphi'}{\sin m'}, \text{ so } \sin m' = \frac{\sin\varphi'}{\sin\varphi}\sin m, \quad (3)$$

$$\cos A = \frac{\cos\varphi\sin(\beta-90)}{\sin m} = \frac{\cos\varphi'\sin(270-\beta')}{\sin m'}, \text{ so}$$

$$\sin m = \frac{\cos\varphi\sin(\beta-90)}{\cos\varphi'\sin(270-\beta')}\sin m' \quad (4)$$

$$\cos m = \cos\varphi\cos(\beta-90) = \cos\varphi\sin\beta \quad (5)$$

$$\cos m' = \cos\varphi'\cos(270-\beta') = -\cos\varphi'\sin\beta'. \quad (6)$$

From Fig. 3(c):

$$\sin m = \sin m'\sqrt{\lambda} \quad (7)$$

$$\lambda = 1 + \gamma^2\sin^2\varphi - 2\gamma\sin\varphi\cos m. \quad (8)$$

Combining (8) and (5):

$$\lambda = \gamma^2\sin^2\varphi - 2\gamma\sin\varphi\cos\varphi\sin\beta + 1. \quad (9)$$

Combining (7) and (3):

$$\sin m = \sqrt{\lambda}\frac{\sin\varphi'}{\sin\varphi}\sin m, \text{ or } \sin\varphi' = \frac{\sin\varphi}{\sqrt{\lambda}}$$

$$\varphi' = \sin^{-1}\frac{\sin\varphi}{\sqrt{\lambda}} \quad (0 \leq \varphi' \leq 90). \quad (10)$$

Combining (7) and (4): $\cos\varphi\sin(\beta-90) = \cos\varphi'\sin(270-\beta')\sqrt{\lambda}$.
Using normal trigonometric transformations:

$$\frac{\beta'}{360-\beta'} = \cos^{-1}\frac{\cos\varphi\cos\beta}{\cos\varphi'\sqrt{\lambda}} \quad (11)$$

Whether equation (11) gives the value of β' or of $360-\beta'$ is seen from the sign of $\sin\beta'$: when $\sin\beta'$ is positive equation (11) gives β', if it is negative it gives $360-\beta'$. From Fig. 3(c):

$$1 = \gamma^2\sin^2\varphi + \lambda - 2\gamma\sin\varphi\cos m'\sqrt{\lambda}. \quad (12)$$

Substituting $\cos m'$ with $-\cos\varphi'\sin\beta'$ from (6) and rearranging:

$$\sin\beta' = \frac{1-\gamma^2\sin^2\varphi-\lambda}{2\gamma\sin\varphi\cos\varphi'\sqrt{\lambda}}.$$

Combining it with (9), it simplifies to:

$$\sin\beta' = \frac{\cos\varphi\sin\beta - \gamma\sin\varphi}{\cos\varphi'\sqrt{\lambda}}. \quad (13)$$

As the denominator is always positive, $\sin\beta'$ is positive for $\cos\varphi\sin\beta > \gamma\sin\varphi$.

When the orientation (β', φ') of the line in the deformed case is known, the original orientation and the elongation it has taken up may be found from the following equations.

From (10):

$$\varphi = \sin^{-1}[\sin\varphi'\sqrt{\lambda}] \quad (14)$$

Combining (12) with (6) and (14) and rearranging:

$$\frac{1}{\lambda} = \gamma^2\sin^2\varphi' + 2\gamma\sin\varphi'\cos\varphi'\sin\beta' + 1. \quad (15)$$

From (11):

$$360 - \frac{\beta}{\beta} = \cos^{-1}\frac{\cos\beta'\cos\varphi'\sqrt{\lambda}}{\cos\varphi}. \quad (16)$$

From (13) combined with (10):

$$\sin\beta = \frac{\sin\beta'\cos\varphi'\sqrt{\lambda} + \gamma\sin\varphi'\sqrt{\lambda}}{\cos\varphi}.$$

If $\sin\beta'\cos\varphi' + \gamma\sin\varphi' > 0$, equation (16) gives β.

Equation (15) may be rewritten to:

$$\sin\beta' = \frac{1/\lambda - \gamma^2\sin^2\varphi' - 1}{2\gamma\sin\varphi'\cos\varphi'} \quad (17)$$

From Fig. 3(c):

$$\gamma^2\sin^2\varphi = \lambda + 1 - 2\cos\omega\sqrt{\lambda}$$

$\cos\omega = \frac{\lambda + 1 - \gamma^2\sin^2\varphi}{2\sqrt{\lambda}}$. Combining with (9):

$$\cos\omega = \frac{1 - \gamma\sin\varphi\cos\varphi\sin\beta}{\sqrt{(\gamma^2\sin^2\varphi - 2\gamma\sin\varphi\cos\varphi\sin\beta + 1)}}. \quad (18)$$

TWO-DIMENSIONAL STRAIN IN A RANDOMLY ORIENTED PLANE

From triangle *ABC* (Fig. 6) where $\angle A = 2\theta'$, $< C = 180 - p'$ and the side $AC = v$ for plane *CBC'* when $v \geq 90$, and $180 - v$ when $v \leq 90$:

$$\sin B = \frac{\sin 2\theta'\sin v}{\sin a}. \quad (19)$$

$$\cos B = -\cos 2\theta'\cos(180-p') - \sin 2\theta'\sin(180-p')|\cos v|. \quad (20)$$

$$\cos a = \frac{\cos 2\theta' + \cos B\cos(180-p')}{\sin B\sin(180-p')}. \quad (21)$$

Substituting (19) and (20) in (21) and rearranging:

$$\frac{\tan a}{\cot 2\theta'} = \frac{\sin(180-p')\sin v}{-\cot 2\theta'\cos^2(180-p') - \sin(180-p')\cos(180-p')|\cos v|}. \quad (22)$$

Using $2\theta' = \tan^{-1}\frac{2}{\gamma}$ (*p.*) and dividing by two, (22) simplifies to:

$$\left.\begin{matrix}\frac{a}{2}\\ \frac{a}{2} - 90\end{matrix}\right\} = \frac{1}{2}\tan^{-1}\left[\frac{\sin(180-p')\sin\hat{v}}{\gamma/2\,(1-\cos^2(180-p')) - \sin(180-p')\cos(180-p')|\cos v|}\right]. \quad (23)$$

If the figure in the square brackets is positive, equation (23) gives $\frac{a}{2}$; if it is zero, $\frac{a}{2} = 0$ for $180 - p' > 2\theta'$ and $^a = 90$ for $180 - p' < 2\theta'$. If the figure in the square brackets is negative, equation (23) gives $\frac{a}{2} - 90$.

To find the orientation (β', φ') of X_P, a plane containing the c-kinematic-axis and X_P is drawn to cut the ab-plane in L (Fig. 6).
$LA = \beta' - 180$
$LC = v - \beta' + 180$ for $v \geq 90$, $p' > 90$ and for $v < 90$, $p' < 90$
$LC = \beta' - 180 - v$ for $v < 90$, $p' > 90$ and for $v \geq 90$, $p' < 90$

$\angle LCX_P = 180 - p'$ for $p' > 90$ and p' for $p' < 90$.
From triangle CX_PL:

$$\varphi' = \sin^{-1}\left[\sin (180 - p') \sin \frac{a}{2} \cdot\right] \tag{24}$$

$$\beta' = \pm \sin^{-1}\left[\frac{\cos (180 - p') \sin \frac{a}{2}}{\cos \varphi'}\right] + v + 180. \tag{25}$$

For $v > 90$ the sign in front of the $\sin^{-1}$ is negative, for $v \leq 90$ it is positive.

Similarly the orientation (β', φ') for Y_P, the maximum finite shortening direction in the plane, is found from triangle $C'MY_P$ (Fig. 6):

$$\varphi' = \sin^{-1}\left[\sin (180 - p') \sin (90 - \frac{a}{2})\right]. \tag{26}$$

$$\beta' = \pm \sin^{-1}\left[\frac{\cos (180 - p') \cos \frac{a}{2}}{\cos \varphi'}\right] + v. \tag{27}$$

Here the sign in front of the $\sin^{-1}$ is negative for $v \leq 90$.

The value of stretching and shortening $\sqrt{\lambda}$ of X_P and Y_P are found by putting the values of β' and φ' into equation (15).

As the deformation is non-dilatational $\sqrt{\lambda_{X_P}} \sqrt{\lambda_{Y_P}} t = 1$, where t is the thickness of a layer with initial thickness 1, and where $\sqrt{\lambda_{X_P}}$ and $\sqrt{\lambda_{Y_P}}$ are measured in the layer surface. t is then found from:

$$t = \frac{1}{\sqrt{\lambda_{X_P}} \sqrt{\lambda_{Y_P}}}. \tag{28}$$